



e-ISSN: 2319-8753 | p-ISSN: 2347-6710

# IJRSET

International Journal of Innovative Research in  
**SCIENCE | ENGINEERING | TECHNOLOGY**

# INTERNATIONAL JOURNAL OF INNOVATIVE RESEARCH

IN SCIENCE | ENGINEERING | TECHNOLOGY

Volume 12, Issue 9, September 2023

**ISSN** INTERNATIONAL  
STANDARD  
SERIAL  
NUMBER  
INDIA

Impact Factor: 8.423

 9940 572 462

 6381 907 438

 [ijirset@gmail.com](mailto:ijirset@gmail.com)

 [www.ijirset.com](http://www.ijirset.com)

# ANFIS Based Direct Torque Control Topology for Double Stator Machine

B. JANSHI<sup>1</sup>, Smt M. SHIRISHA<sup>2</sup>, Ms S. ANUSHA<sup>3</sup>

<sup>1</sup>Post Graduate Student, JNTUA College of Engineering, Anantapuramu, India

<sup>2</sup>Assistant Professor (Adhoc), JNTUA College of Engineering, Anantapur, India

<sup>3</sup>Assistant Professor (Adhoc), JNTUA College of Engineering, Anantapur, India

**ABSTRACT-** This paper presents a Direct Torque Control (DTC) Topology of a Double Stator Machine (DSM). In the renewable energy system and the Electric Vehicle (EV) traction system, for high torque and low speed application the dual stator machine is suitable. In proposed Fuzzy DTC method there are many fluctuations in the speed performances, flux evolution, and the total electromagnetic torque ( $C_e$ ) progress. These drawbacks can be resolved by an improved Adaptive Neuro Fuzzy Inference System (ANFIS) controller to improve and control the speed, torque of a dual stator machine and supervise the two stator fluxes and currents. In the proposed method DTC topology and the field oriented vector control were utilized to control the torque, speed of the dual stator machine. MATLAB/SIMULINK software is developed to study the various dynamic response of the speed, torque, flux and the currents of double stator machine and shows the behaviour of the output results.

**KEYWORDS:** Direct torque control (DTC), Fuzzy logic controller (FLC), vector modulation, Adaptive neuro fuzzy inference system (ANFIS), MATLAB/SIMULINK, Simulation results.

## I. INTRODUCTION

Till date, All manufacturing processes and production lines require dual stator machines. Recently, it has been included into electrical transportation technologies like electric vehicles and the field of renewable energy (EV). For some of these applications, a tiny motor with a high torque factor is required, while others call for a high power efficiency at low speeds. In order to address some of these issues, permanent magnet machines as well as dual stator and dual rotor machines were developed. The dual stator machine provided some solutions when focused on low wind speed in particular circumstances and on electric car applications and efficiency, which need for a high-power machine with a small dimension. Early in the 20th century, two stator machines were developed [1]. Lipo and Muouz [2]. Those advantages stem from the potential for an expanded operating range, which includes low-speed operation and complete stator winding usage [3]. Control techniques were put up to solve this issue. As described in [4]–[6], these control loops were based on pulse-width modulation systems. The stator 1 and stator 2 are two-three phase stator windings, and the rotor winding is a common squirrel-cage winding in a dual stator induction machine. The two stators feature two different pairs of poles and can be moved apart by one angle. The stator poles are typically chosen in a 1:3 ratio (for example, 2:6 or 4:12) [7]. Because of this, the stator arrangement is ideal for traction drive propulsion and generation systems in automobiles and other applications where durability is of utmost importance. The Direct Torque Control (DTC) method, which is used for three-phase induction motors, can be applied to dual stator machines as well [13, 14], as can the field-oriented vector control loop. For these induction machines, the direct torque control, which directly regulated the torque, was more reliable and simple. The Direct Torque Control uses a basic architecture that hysteresis controllers, shown numerous peaks and valleys in the output variables, including the magnetic torque, speed, and magnet flux.

Direct torque control (DTC) system created for machine control for a twin stator. At first, the relevant equations were given along with study and modelling of the motor system. The matching ANFIS controllers were then created after using the ANFIS controller to improve this control topology method. Therefore, focusing on twelve sectors appears to reduce flux and torque ripples. Additionally, modifying the hysteresis control parameters online while evaluating the efficiency of the optimization algorithms might produce even better results. The effectiveness of the suggested strategy was assessed using the Matlab/Simulink program.



**A. MODELLING OF DUAL STATOR MACHINE:**

To define all the inputs, variables, and parameters in a dual stator machine, a physical system's control must go through the modelling step. Given that connected windings rotors and twin stator machine three phase stators are both present, the following mathematical models will be defined:

1.ELECTRICAL EQUATIONS

The dual stator machine's mathematical equations can be expressed as follows with a fixed reference to the stator:

Equations for the complex vector variable of the stator and rotor voltage and flux are provided (1).

$$\begin{cases} vs1 = rs1is1 + p\phi s1 \\ vs2 = rs2is2 + p\phi s1 \\ rrir + p\phi r = 0 \end{cases} \quad (1)$$

Equations for the corresponding fluxes are shown in the equation (2)

$$\begin{cases} \phi s1 = Ls1is1 + Ls1rir1 \\ \phi s2 = Ls2is2 + Ls2rir2 \end{cases} \quad (2)$$

The equation can be used to express the stator inductance (3). It is crucial to mention that equation can be used to define I [1,2] and the inductance of the rotor faces of the two stators (4). The number of rotor winding spins for the first or second stator influences, respectively, is an or xn.

$$Lsi = \begin{bmatrix} Llsi + Lmsi & -\frac{Lmsi}{2} & -\frac{Lmsi}{2} \\ -\frac{Lmsi}{2} & Llsi + Lmsi & Llsi + Lmsi \\ Llsi + Lmsi & -\frac{Lmsi}{2} & Llsi + Lmsi \end{bmatrix} \quad (3)$$

$$Lslr = \begin{bmatrix} La1 & La2 & \dots & La(n-1) & Lan \\ Lb1 & Lb2 & \dots & Lb(n-1) & Lbn \\ Lc1 & Lc2 & \dots & Lc(n-1) & Lcn \end{bmatrix}$$

$$Ls2r = \begin{bmatrix} Lx1 & Lx2 & \dots & Lx(n-1) & Lxn \\ Ly1 & Ly2 & \dots & Ly(n-1) & Lyn \\ Lz1 & Lz2 & \dots & Lz(n-1) & Lzn \end{bmatrix} \quad (4)$$

Values of inductances and the angle between the teeth and the poles. Equation (2) can therefore also be expressed in this way (5).

$$\begin{cases} \phi s1 = \left(Ls1l + \frac{3}{2}Lms1\right) is1 + \frac{n}{2}Lmejp1(\theta r + \delta)ir1 \\ \phi s2 = \left(Ls1l + \frac{3}{2}Lms2\right) is2 + \frac{n}{2}Lmejp2(\theta r + \delta)ir2 \end{cases} \quad (5)$$

This will enable a new interpretation of the stator voltages and equations (6), which are given in the new form as

$$\begin{cases} vs1 = rs1is1 + \left(Lls1 + \frac{3}{2}Lms1\right) pis1 + \frac{n}{2}Lm1ejp1(\theta r + \delta)(p + jp1\omega1)ir1 \\ vs2 = rs2is1 + \left(Lls1 + \frac{3}{2}Lms2\right) pis2 + \frac{n}{2}Lm2ejp2(\theta r + \delta - \xi)(p + jp2\omega2)ir2 \end{cases} \quad (6)$$

If focusing on the rotor side, the expression for the flux vectors may be written as equation (7), while the statement for the rotor voltages can be written as equation (8).

$$\begin{cases} \phi_{r1} = Lr1ir1 + \frac{3}{2}Lm1e - jp1(\theta r + \delta)is1 \\ \phi_{r2} = Lr2ir2 + \frac{3}{2}Lm2e - jp2(\theta r + \delta - \xi)is2 \end{cases} \quad (7)$$

$$\begin{cases} 0 = rr1ir1 + \frac{3}{2}Lm1e - jp1(\theta r + \delta)(p - jp1\omega r)is1 \\ 0 = rr2ir2 + \frac{3}{2}Lm2e - jp2(\theta r + \delta - \xi)(p - jp2\omega r)is2 \end{cases} \quad (8)$$

Equation (9), which summarises the new voltage equations, and equation (11), which summarises the related flux equations (10).

$$\begin{cases} vqds1 = rs1iqds1 + jp1\omega1\phi qds1 + p\phi qds1 \\ vqds2 = rs2iqds2 + jp\omega2\phi qds2 + p\phi qds2 \\ 0 = rr1iqdr1 + jp1(\omega1 - \omega r)\phi qdr1 + p\phi qdr1 \\ 0 = rr2iqdr2 + jp2(\omega2 - \omega r)\phi qdr2 + p\phi qdr2 \end{cases} \quad (9)$$

Where:

$$\begin{cases} \phi qds1 = (Ls1 - Lm1)iqds1 + Lm1(iqds1 + iqdr1) = Ls1iqds1 + Lm1iqdr1 \\ \phi qds2 = (Ls2 - Lm2)iqds2 + Lm2(iqds2 + iqdr2) = Ls2iqds2 + Lm2iqdr2 \\ \phi qdr1 = (Lr1 - Lm1)iqdr1 + Lm1(iqdr1 + iqds1) = Lr1iqdr1 + Lm1iqds1 \\ \phi qdr2 = (Lr2 - Lm2)iqdr2 + Lm2(iqdr2 + iqds2) = Lr2iqdr2 + Lm2iqds2 \end{cases} \quad (10)$$

With  $\omega_1$  and  $\omega_2$  is the rotor's electrical speed, and  $r$  is the rotor speed.  $vqds1$ ,  $vqds2$ ,  $vqdr1$  and  $vqdr2$  are stator and rotor q-d axis voltages.  $iqds1$ ,  $iqds2$ ,  $iqdr1$  and  $iqdr2$  are stator and rotor q-d axis currents.  $\phi qds1$ ,  $\phi qds2$ ,  $\phi qdr1$  and  $\phi qdr2$  are stator and rotor q-d axis flux and  $P=Dd/dt$ .  $Lm1$  and  $Lm2$  is the magnetizing inductance, and  $Lr1$ ,  $Lr2$ ,  $Ls1$  and  $Ls2$  are rotor inductances.

## II. MECHANICAL EQUATIONS

The interaction between the electromagnetic fields of the stator 1 and rotor and the stator 2 and rotor combine to form the total electromagnetic torque ( $C_e$ ), which is made up of two components. This relation can be found in equation (11).

$$C_e = \frac{3}{2}p1Im[\phi qds1 iqds1] + \frac{3}{2}p2Im[\phi qds2 iqds2] \quad (11)$$

When the DSM roto mechanical speed is related to the electromagnet torque and load, it may be expressed using the dual stator machine's fundamental dynamic equation, as shown in equation (12). The inertia factor is  $J$ , while the friction factor is  $B_s$ .

$$\omega_m = \frac{C_e - Cl}{(J_s + B_s)} \quad (12)$$

## B. DIRECT TORQUE CONTROL (DTC) OF INDUCTION MACHINE

By choosing the best switching modes for the inverters, it is a method that enables direct and personalised control of the motor torque. The basic motor inputs, such as the stator voltages and currents, are used to calculate the electromagnetic torque and stator flux in the beginning. This control's main objective is to control the stator flux and electromagnetic torque without measuring speed, flux, or torque other than voltage and current measurements.

## III. STATOR FLUX, ELECTROMAGNET TORQUE, AND SECTOR ESTIMATION MODEL

The mathematical models that were utilised to estimate the fluxes and electromagnet torque must be expressed. It is possible to assess the expressions of the two fluxes into the two stators as it is in equations (13) to (15)

$$\begin{cases} \phi_{s1} = \sqrt{\phi_{2s1\alpha}^2 + \phi_{2s1\beta}^2} \\ \phi_{s2} = \sqrt{\phi_{2s2\alpha}^2 + \phi_{2s2\beta}^2} \end{cases} \quad (13)$$

Where all the variables in equation (13) were given in (14) and (15)

$$\begin{cases} \phi_{s1\alpha} = \int_0^t (u_{s1\alpha} + R_{s1}i_{s1\alpha}) dt \\ \phi_{s1\beta} = \int_0^t (u_{s1\beta} + R_{s1}i_{s1\beta}) dt \end{cases} \quad (14)$$

And

$$\begin{cases} \phi_{s2\alpha} = \int_0^t (u_{s2\alpha} + R_{s2}i_{s2\alpha}) dt \\ \phi_{s2\beta} = \int_0^t (u_{s2\beta} + R_{s2}i_{s2\beta}) dt \end{cases} \quad (15)$$

where  $\phi_{s1\alpha}, \phi_{s2\alpha}, \phi_{s1\beta}$  and  $\phi_{s2\beta}$  represents the flux stators according to the axes  $(\alpha, \beta)$ .  $u_{s1\alpha}, u_{s2\alpha}, u_{s1\beta}$  and  $u_{s2\beta}$  represents the voltages stators according to the axes  $(\alpha, \beta)$  and  $i_{s1\alpha}, i_{s2\alpha}, i_{s1\beta}$  and  $i_{s2\beta}$  represent the currents stators according to the axes  $(\alpha, \beta)$ . So, the estimation of the angles of the first and second stators noted, respectively,  $\theta_{s1}$  and  $\theta_{s2}$  is calculated from equation (16).

$$\begin{cases} \theta_{s1} = \arctg \frac{\phi_{s1\beta}}{\phi_{s1\alpha}} \\ \theta_{s2} = \arctg \frac{\phi_{s2\beta}}{\phi_{s2\alpha}} \end{cases} \quad (16)$$

On the other hand, the electromagnet torque estimation can be assessed as it is represented in equation (17).

$$C_e = p \frac{L_m}{L_r} K \phi_{s1} \phi_r \sin \delta \theta_1 + p \frac{L_m}{L_r} K \phi_{s2} \phi_r \sin \delta \theta_2 \quad (17)$$

In above equation K is a symbol for the motor constant.  $\delta \theta_1$ , and  $\delta \theta_2$ , the angles between the stator (1), stator (2) and, correspondingly, the rotor flux vector.

### C. THE FUZZY DTC ARCHITECTURE

Within the Fuzzy DTC architecture, the conventional direct torque control loop and the fuzzy logic controller were built and put into use. In terms of managing a twin stator machine, the architecture also performs better. When the machine is in motor mode, torque, flux ripples, and poor motor performance are eliminated to improve the controlling solution. Based on the benefit

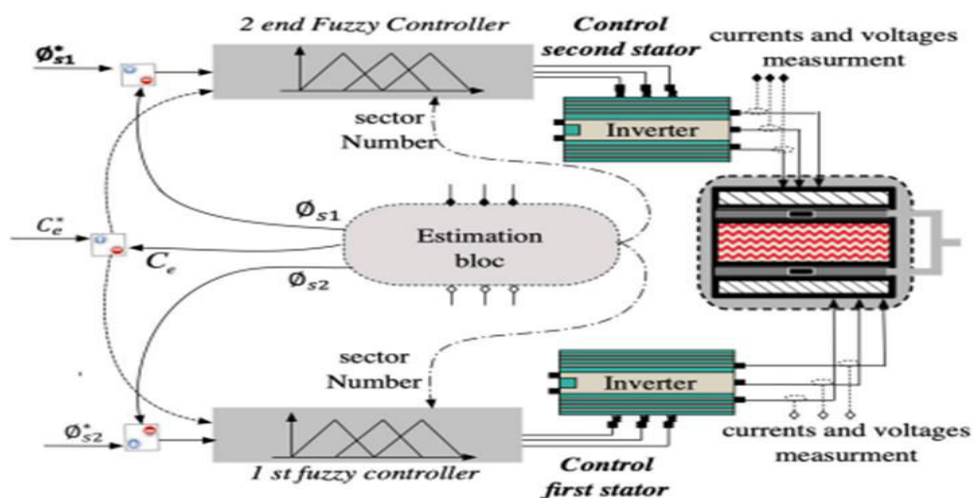


Figure 1: The scheme of the Fuzzy-DTC control loop



Another version of the fuzzy logic controller's DTC is created utilising fuzzy controllers to address the hysteresis problem. The modified DTC loop's basic operating principle is now based on two fuzzy controllers, each of which makes use of the differences between the real and reference flux and magnetic torque as well as the predicted angular positions of each stator relative to the rotor. Each of these fuzzy controllers will simultaneously bear sole responsibility for the switching table outputs. This building is created in figure :1

**1. THE FUZZIFICATION STEP**

In the fuzzification step the fuzzy controller will directly manage the switching table loop, the flux error position for the first stator (ø<sub>s1</sub>), as well as the second stator (ø<sub>s2</sub>), both the mistaken electromagnetic torque (C<sub>e</sub>) shall be fuzzified. The triangle function type is chosen, and three membership functions for each of these variables are chosen. The third input parameter of the fuzzy controller, which pertains to the first and second flux positions, is instead chosen from six membership functions. Table (1) enumerates each of these membership features.

Fuzzy sets	Small (S)	Null(N)	Large(L)
Flux 1 error	<-1	-1<<1	1<
Flux2 error	<-0.5	-0.5<<0.5	0.5<
Torque error	<-30	-30<<30	30<

Fuzzy sets	Forth	Fifth	Sixth	First	Second	Third
Flux1 angle	<-2or2<	-3<<-1	-2<<0	-1<<1	0<<2	1<<3
Flux2 angle	<-2or2<	-3<<-1	-2<<0	-1<<1	0<<2	1<<3

Table :1 Fuzzy sets for each input variable

**2. THE DEFUZZIFICATION STEP**

According to the three switches on each of the two employed inverters, the output variables are split into three binary outputs. The statues of each switcher are thus represented by two fuzzy sets.

**3. THE RULES**

The Mamdani method is the inference method utilised with the 54 fuzzy rules created for this upgraded DTC architecture. With the fifth angular point chosen, Fig. 2 illustrates the scenario for all the rules.

First flux angle in the Fifth set

**Flux 1error**

	S	N	L
S	(001)	(000)	(010)
N	(101)	(111)	(110)
L	(111)	(100)	(010)

S1=1, S4=0	S1=1, S4=0
S2=1, S5=0	S2=0, S5=1
S3=1, S6=0	S3=0, S6=1

Fig: 2 if the fifth angular position is chosen, the switches are combined to feed the first stator.

Table (2) combines together all of the first stator feeding rules, while Table (3) displays the second stator part's specified rules. It is crucial to note that because two distinct stators will be regulated, the two tables will not display the



same rules. Consider the scenario where the specifications of the two stators are the same. The two controllers could then use the same rules, or there could be only one fuzzy controller that could control both stators simultaneously. No independence between the two stators is possible in this situation.

Rules	Input vector			Output(s1,s2,s3)
	Flux error	Torque error	Flux1 angle	
R1	Small	Small	First	000
R2	Small	Small	Second	010
R3	Small	Small	Third	011
R4	Small	Small	Fourth	110
R5	Small	Small	Fifth	001
R6	Small	Small	Sixth	101
R7→R48				
R49	Large	Large	First	101
R50	Large	Large	second	010
R51	Large	Large	Third	111
R52	Large	Large	Fourth	011
R53	Large	Large	Fifth	011
R54	Large	Large	Sixth	100

Table:2 The 54 rules description for feeding the first stator

Rules	Input vector			Output (s1,s2,s3)
	Flux2 error	Torque error	Flux2 angle	
R1	Small	Small	First	010
R2	Small	Small	Second	011
R3	Small	Small	Third	001
R4	Small	Small	Fourth	110
R5	Small	Small	Fifth	100
R6	Small	Small	Sixth	001
R7→R48				
R49	Large	Large	First	101
R50	Large	Large	Second	111
R51	Large	Large	Third	110
R52	Large	Large	Fourth	100
R53	Large	Large	Fifth	000
R54	Large	Large	Sixth	011

Table: 3 The 54 rules description for feeding the second stator.

D.SIMULATION ANALYSIS

In this paper The twin stator machine findings have been tested using the simulations of the DTC control topology that are supplied. Both stator one and stator two were created utilising the 3-hp induction machine's design parameters. Table lists the specs for dual stator machines (4). We will evaluate the performance of the Fuzzy DTC control loop and the ANFIS controller in the simulation test. A load torque will be delivered at the occasion of 0.4 seconds after the reference motor speed is initially offered for touching 150rad/s as a ramp form. The simulation test is carried out within

A total of two seconds equals one time. Previously, the hysteresis bounds for the fluxes and electromagnet torque in the traditional DTC control loop were 0.005 Wb and 0.5N.m, respectively.

### 1. UNCONTROLLABLE DSM

The findings are depicted in Figure 3 for the no-load operation "Cr=0," for the time intervals of 0 to 0.4 seconds, and for a nominal speed value of 188.5 rad/s. The total electromagnetic torques show that as well. If no control loop is activated, the motor speed will decrease and the currents will rise starting at 0.4 seconds when a load torque of "Cr=20N.m" is applied. Fig. 3.c will display the electromagnet torques.

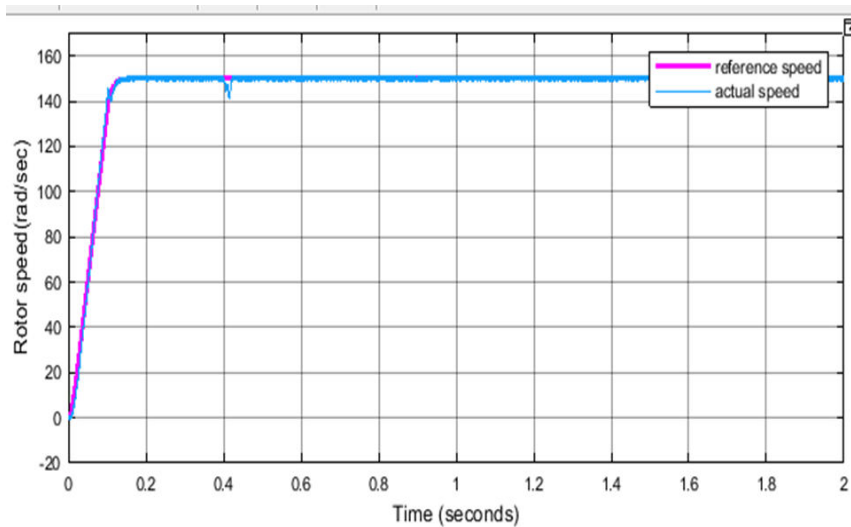


Figure 3: Speed evolution with Fuzzy the DTC architecture.

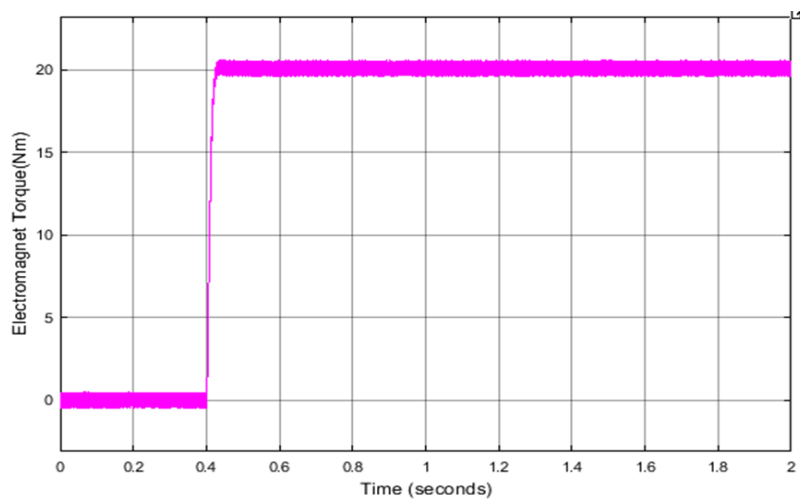


Fig 3.a : Total electromagnetic torque response using a fuzzy DTC architecture.

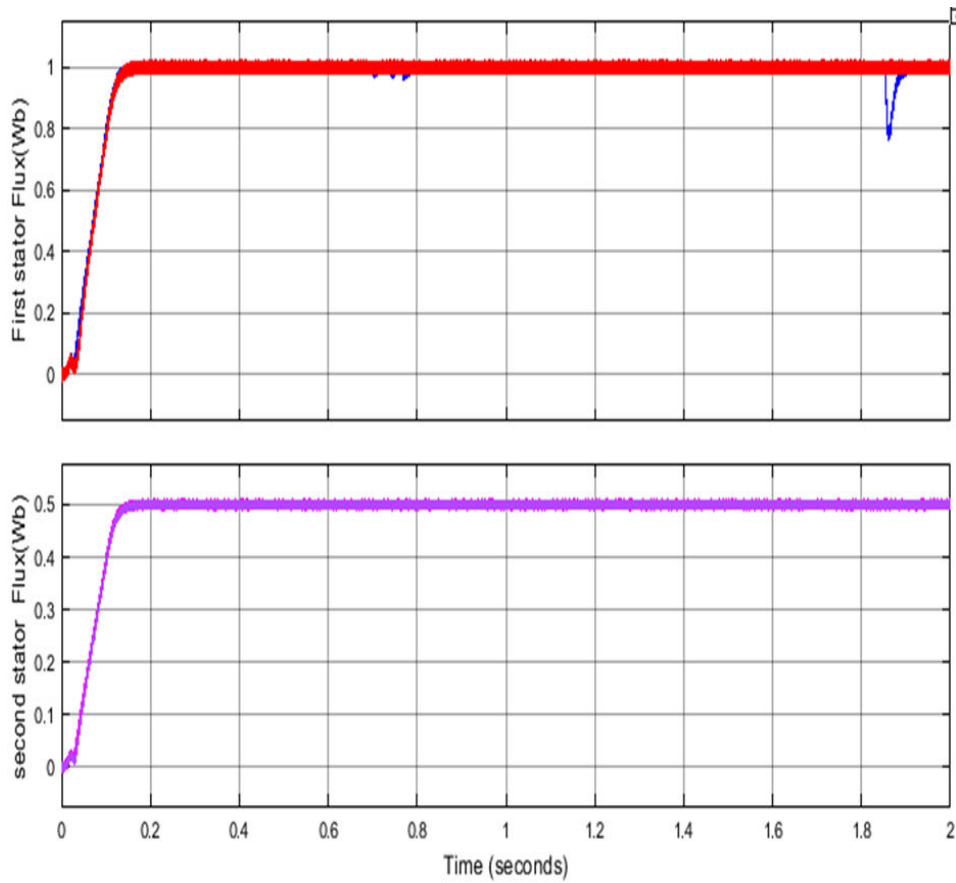


Fig 4: First stator flux response ( $\phi_{s1}$ ), two-stator flux ( $\phi_{s2}$ ), Fuzzy DTC and evolution architecture.

## 2. CONTROLLABLE DSM

The twin stator machine will be controlled using the direct torque control loop described in the preceding sections. the reference speed ramp shape in fig 3.a 150rad/s which is the nominal speed during the simulation's whole runtime. 0.4 seconds later. When compared to the traditional DTC form, the reaction time with fuzzy DTC performs better. Also, Stator currents operate well in the Fuzzy DTC version, as demonstrated in the fig 4. In the fig 4, Since there is only one phase of the current displayed, it is evident that all of the current's oscillations and ripples have been removed. The fig 5 provides good results for the currents in the second stator, and it appears that many current variations were minimised by the use of the fuzzy DTC topology.

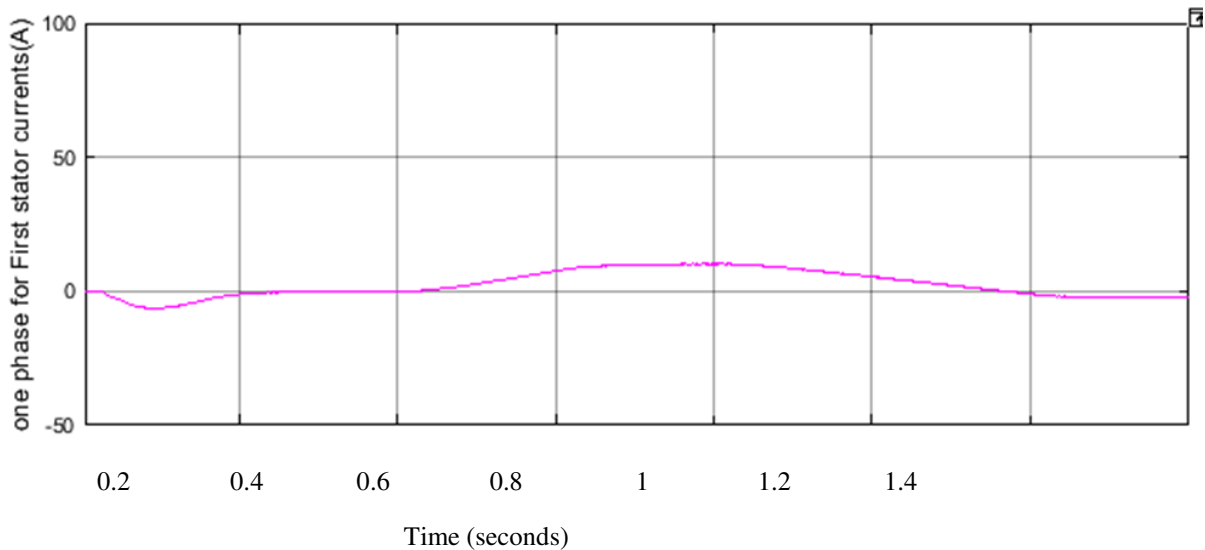


Fig 5: Response of the one phase current(A), for the first stator, with two DTC architecture.

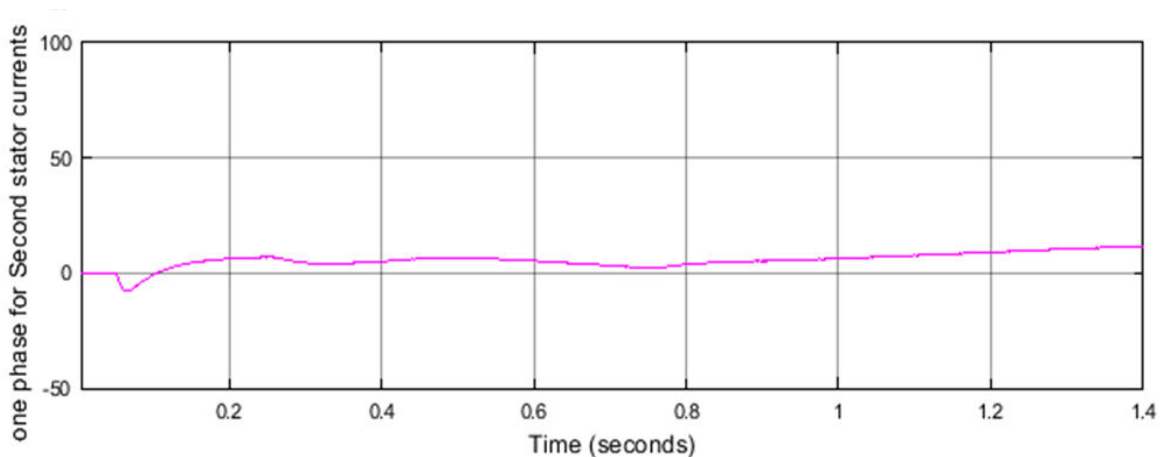
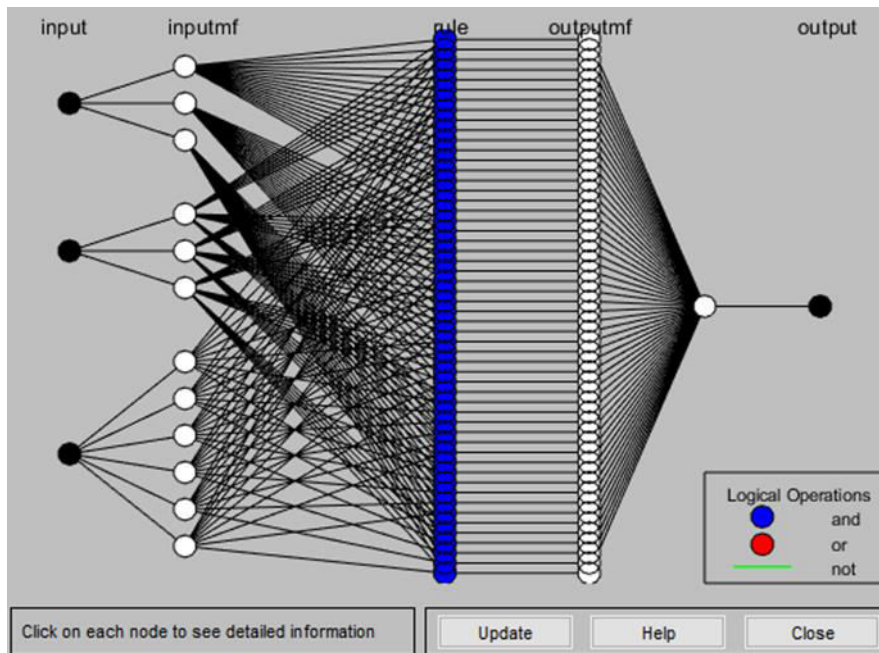


Fig 6: one-phase current's reaction (A), two DTC architecture for the second stator

focusing once more on the case 0.4 sec. will provide further clarification of the function of the fuzzy table. The list of rules that have been chosen ranges from R7 to R13. For the two stator cases, yes. The above switch combination will be [0 0 1 0 01] for the R7 to R13 of the first stator and [1 10 0 1 1] for the R7 to R13 of the second stator, respectively, if focusing on the A-phase. The established rules in Tables (2) and Table 3 are relevant to this phenomenon (3).

### 3. ANFIS CONTROLLER SIMULATION ANALYSIS

A fuzzy sugeno model called the adaptive neural fuzzy inference system (ANFIS) was included into the framework to speed up the learning and adaptation process. Basic architecture of anfis has two input layers x and y also have one output layer f. With each input having three membership functions, this model can be chosen based on fuzzy rules using either the subtractive clustering technique or the grid partitioning technique and similarly, by the 25 The neural network updates the rules using the back propagation method and gradient descent algorithm using data obtained via clustering or the grid partition base approach.



ANFIS controller Basic structure

From the previous Fuzzy DTC analysis to improve the performance of the Dual Stator Machine focusing on twelve sectors appears to reduce flux and torque ripples. Additionally, modifying the hysteresis control parameters online while evaluating the efficiency of the optimization algorithms might produce even better results. By using the ANFIS controller to reduce the torque and flux errors. Fuzzy DTC and ANFIS controller analysis responses like Reference speed, Torque, Flux and the phase currents are shown in the following figures.

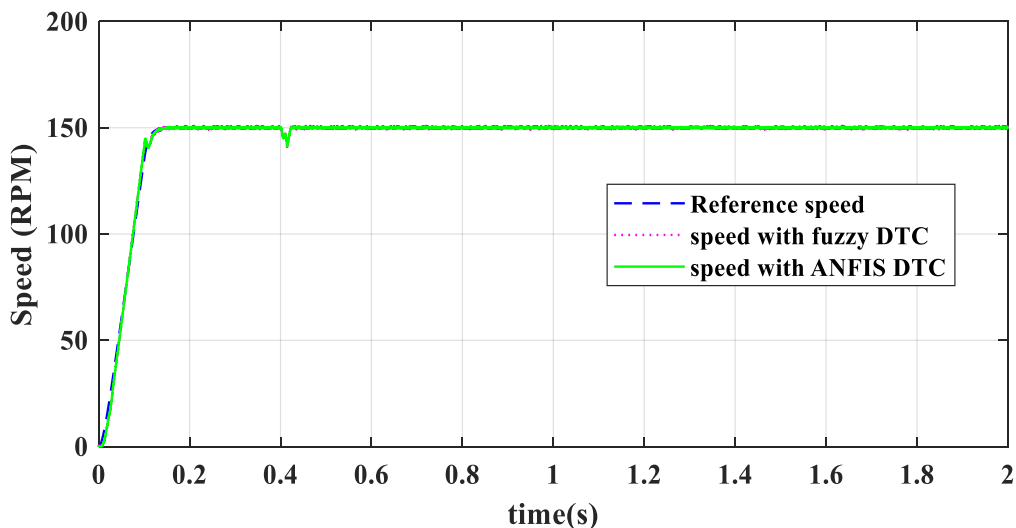


Fig 7: Reference speed evolution with Fuzzy DTC and ANFIS DTC Architecture.

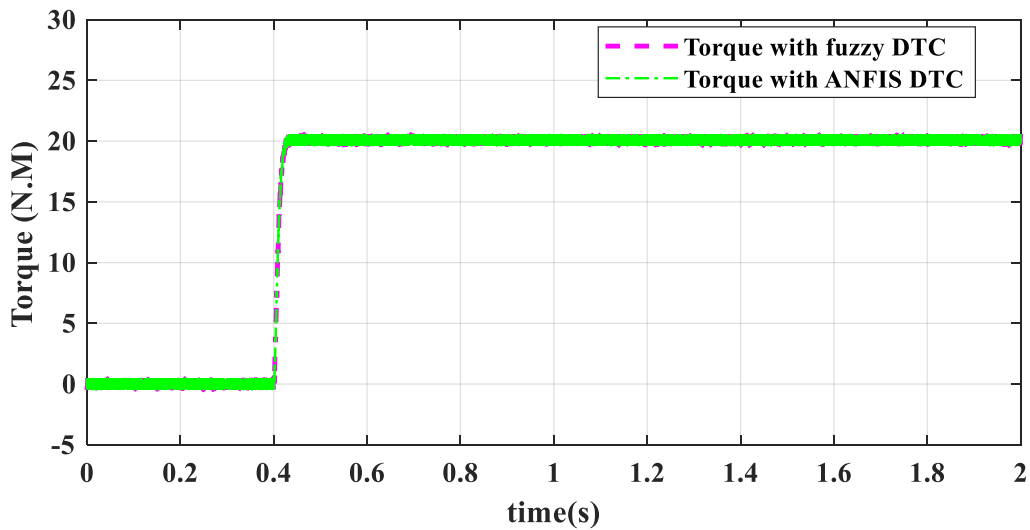


Fig 8: Torque evolution with Fuzzy DTC and ANFIS DTC architecture.

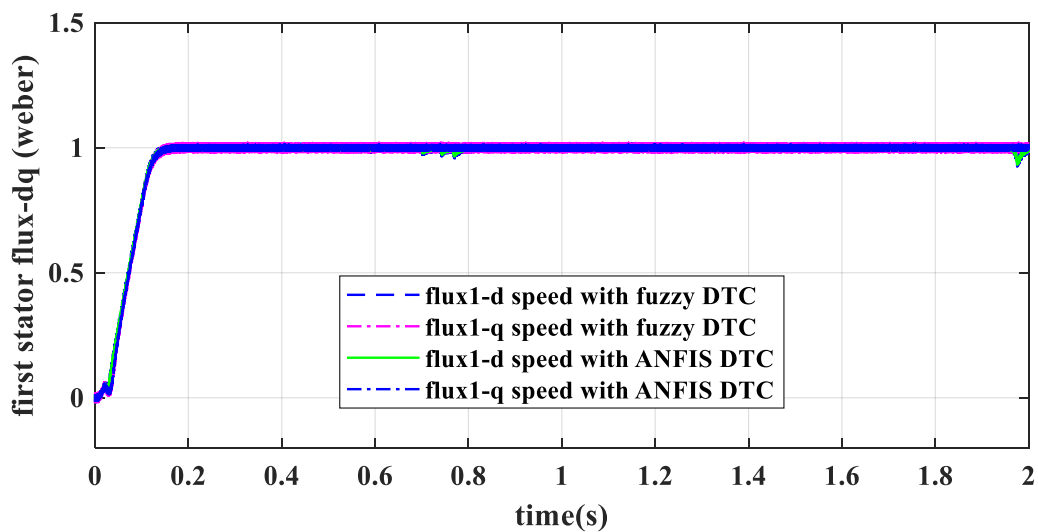
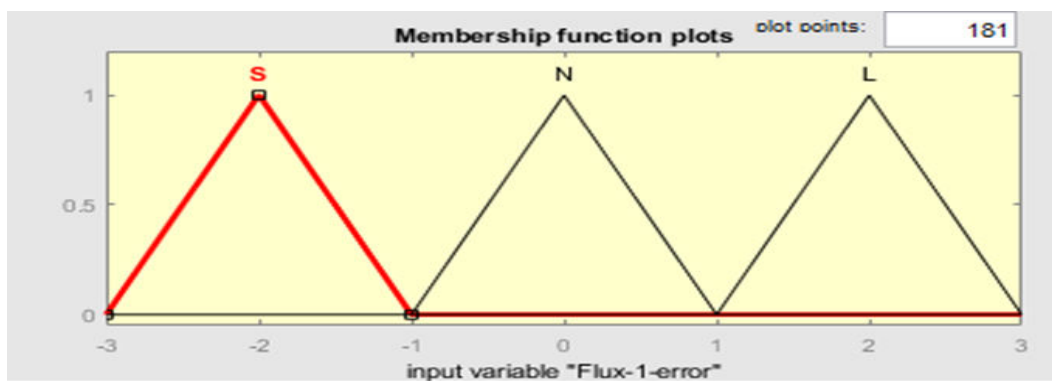
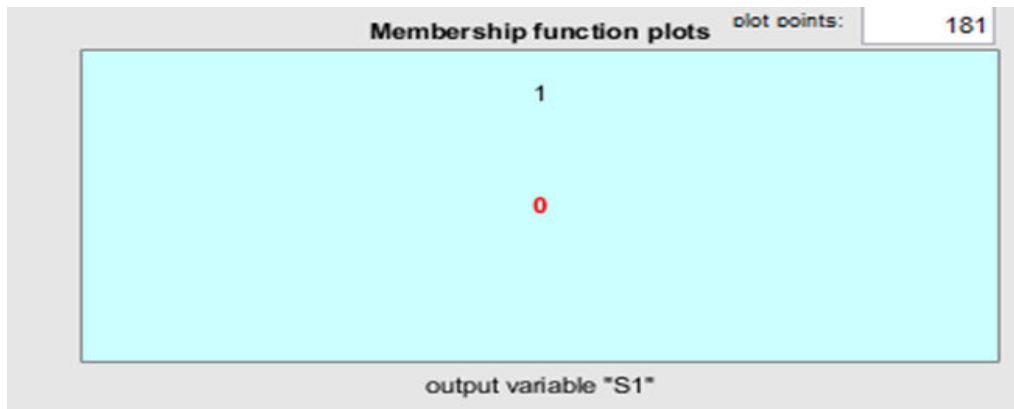


Fig 9: Response of first stator flux( $\phi_{s1}$ ) With Fuzzy DTC and ANFIS DTC architecture.



Flux (1)error



Output for staror 1

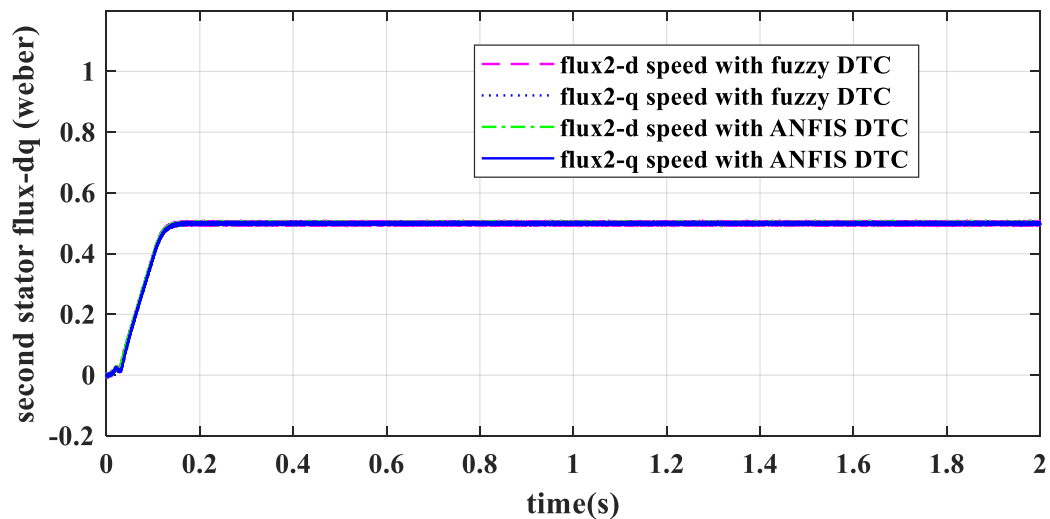
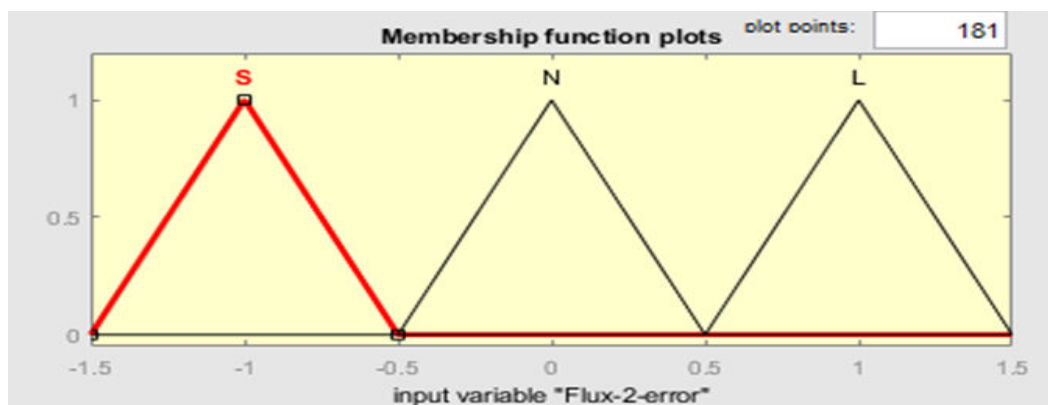
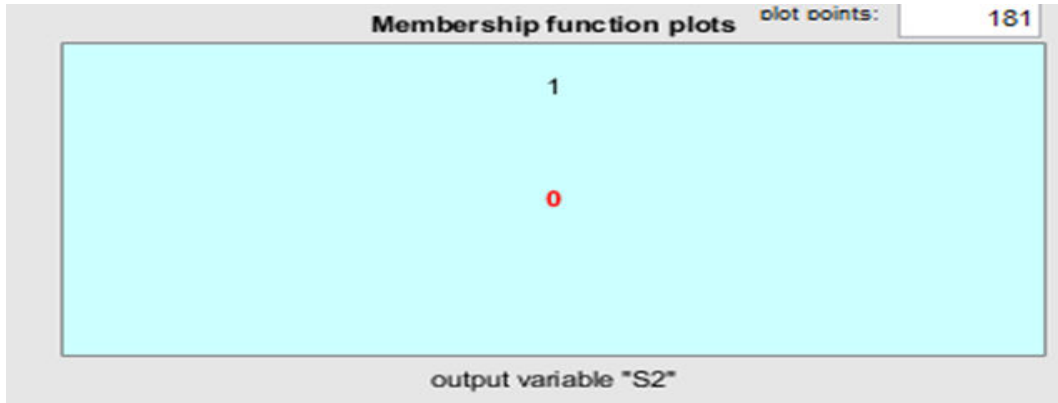


Fig 10: Response of second stator flux ( $\phi_{s2}$ ) with Fuzzy DTC and ANFIS DTC architecture.



Flux 2 error



Output variable for stator 2

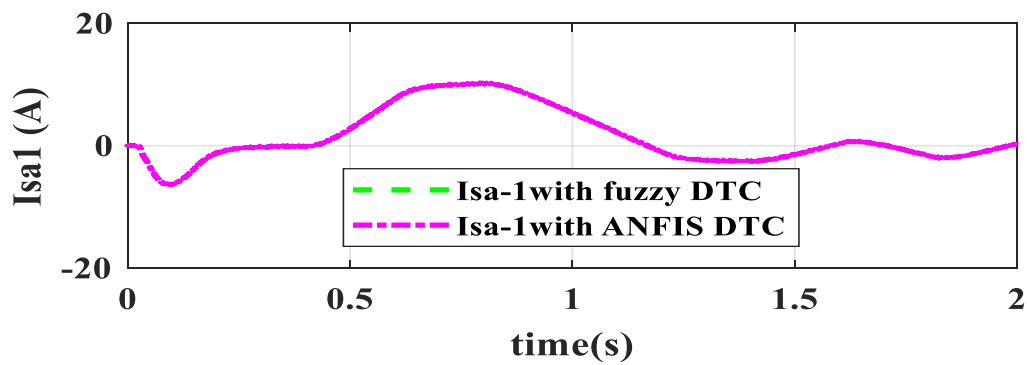


Fig 11: Response of one phase current for the first stator with Fuzzy DTC and ANFIS DTC architecture.

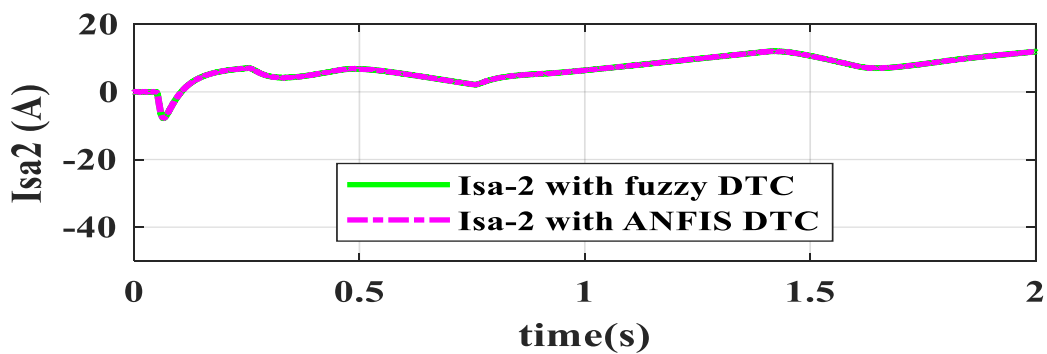


Fig12: Response of one phase current for the second stator with Fuzzy DTC and ANFIS DTC architecture.

#### IV. CONCLUSION

ANFIS based direct torque control (DTC) for dual stator machine has been implemented. The adaptive network based fuzzy inference system (ANFIS) is a data-driven method that simulates a neural network approach to the resolution of function approximation issues. Data-driven techniques for creating ANFIS networks often start with clustering a training set of numerical samples of the unknown function to be approximated. Since its introduction, ANFIS networks have been used to solve problems related to classification, rule-based process management, pattern recognition, and other issues. A fuzzy inference system is comprised in this case of the fuzzy model put forth by Takagi, Sugeno, and Kang to codify a methodical way to generating fuzzy rules from an input output data set. ANFIS controllers were then created after using the FUZZY controller to improve this control topology method. Therefore, focusing on twelve sectors appears to reduce flux and torque ripples. Additionally, modifying the hysteresis control parameters online while evaluating the efficiency of the optimization algorithms might produce even better results. The effectiveness of the suggested strategy was assessed using the Matlab/Simulink program.

#### REFERENCES

- [1] F. Creedy, "Some developments in multi-speed cascade induction motors," *J. Inst. Electr. Eng.*, vol. 59, no. 301, pp. 511\_532, May 1921.
- [2] F. Mehedi, R. Taleb, A. B. Djilali, and A. Yahdou, "SMC based DTCSVM control of  $\pi$ -phase permanent magnet synchronous motor drive," *Indonesian J. Elect. Eng. Comput. Sci.*, vol. 20, no. 1, pp. 100\_108, 2020
- [3] A. M. Lulhe and T. N. Date, "A technology review paper for drives used in electrical vehicle (EV) & hybrid electrical vehicles (HEV)," in *Proc. Int. Conf. Control, Instrum., Commun. Comput. Technol. (ICCCCT)*, Dec. 2015, pp. 632\_636.
- [4] K. Marouani, L. Baghli, D. Hadiouche, A. Kheloui, and A. Rezzoug, "A new PWM strategy based on a 24-sector vector space decomposition for a six-phase VSI-fed dual stator induction motor," *IEEE Trans. Ind. Electron.*, vol. 55, no. 5, pp. 1910\_1920, May 2008
- [5] G. Wang, M. Yang, L. Niu, X. Gui, and D. Xu, "A static current error elimination algorithm for PMSM predictive current control," *Zhong-guo Dianji Gongcheng Xuebao/Chin. Soc. Electr. Eng.*, vol. 35, no. 10, pp. 2544\_2551, 2015.
- [6] Y. Luo and Z. Ke, "Speed estimation rotor flux vector-controlled induction motor drive with motor resistance parameter identification," *Smart Sci.*, vol. 6, no. 4, pp. 363\_373, 2018.
- [7] A. Shukla and R. Sharma, "Modified DTC with adaptive compensator for low-speed region of induction motor in electric vehicle applications," *Smart Sci.*, vol. 8, no. 3, pp. 101\_116, 2020.
- [13] A. R. Munoz and T. A. Lipo, "Dual stator winding induction machine drive," *IEEE Trans. Ind. Appl.*, vol. 36, no. 5, pp. 1369-1379, Sep. 2000.
- [14] J. M. Guerrero and O. Ojo, "Total airgap flux minimization in dual stator winding induction machines," *IEEE Trans. Power Electron.*, vol. 24, no. 3, pp. 787-795, Mar. 2009.
- [15] U. C. Dikshit and R. K. Tripathi, "Direct torque control for dual three-phase induction motor drives," in *Proc. Students Conf. Eng. Syst. (SCES)*, Mar. 2012
- [16] S. Basak and C. Chakraborty, "Dual stator winding induction machine: Problems, progress, and future scope," *IEEE Trans. Ind. Electron.*, vol. 62, no. 7, pp. 4641-4652, Jul. 2015.
- [17] A. Flah, I. A. Khan, A. Agarwal, L. Sbita, and M. G. Simoes, "Field-oriented control strategy for double-stator single-rotor and double-rotor single-stator permanent



**INNO SPACE**  
SJIF Scientific Journal Impact Factor  
**Impact Factor: 8.423**



**ISSN** INTERNATIONAL  
STANDARD  
SERIAL  
NUMBER  
INDIA



# INTERNATIONAL JOURNAL OF INNOVATIVE RESEARCH

IN SCIENCE | ENGINEERING | TECHNOLOGY

**9940 572 462** **6381 907 438** **ijirset@gmail.com**



[www.ijirset.com](http://www.ijirset.com)

Scan to save the contact details